Regional Environmental Change (2025) 25:33
https://doi.org/10.1007/s10113-025-02367-z

ORIGINAL ARTICLE

Changes in the probability of temporally compound wet and dry events in a warmer world: case study in the Upper Jhelum Basin—South Asia

Rubina Ansari[1,2] · Ana Casanueva[3,4] · Muhammad Usman Liaqat[1] · Giovanna Grossi[1]

Received: 4 May 2024 / Accepted: 12 January 2025 / Published online: 12 February 2025

Abstract
Temporal compound events (TCEs), such as the consecutive occurrence of two complementary extremes of the hydrological spectrum (floods and droughts), exhibit a volatile hydrological cycle that exacerbate the challenges associated with water resources management. This study makes use of bias-corrected climate models output from three modeling experiments (CMIP6, CORDEX, and CORDEX-CORE), to examine moderate to extreme wet and dry events and their temporal compounding over the Upper Jhelum Basin (UJB), under low, medium, and high emission scenarios for two future periods (2040–2059 and 2080–2099). Standardized Precipitation Evapotranspiration Index (SPEI) is used to quantify the meteorological wet and dry events that are the main driver of the hydrologic floods and droughts. The two types of TCEs considered in the current study are wet-to-dry (W-to-D) events and dry-to-wet (D-to-W) events in the adjacent month. Results indicate that (1) under warming conditions, wet and dry events are expected to become more frequent and severe whereas duration of the events exhibits distinct change signals depending on the specific location. (2) The basin is more prone to D-to-W TCEs dominated in the southwest of the region, which was not found to be hotspot historically neither for dry nor for wet extreme events. (3) CORDEX and CORDEX-CORE ensembles show varying climate change signals with no specific spatial pattern whereas the CMIP6 ensemble shows stronger change signals and divides the region into two distinct parts, i.e., northeast and southwest.

Keywords Temporal compound events · Bias correction · CMIP6 · CORDEX · CORDEX-CORE · Climate change

Introduction

Climate change is predicted to accelerate the global hydrological cycle and cause extreme events (floods and droughts) with increasing frequency and severity, pushing the limits of society's capacity to forecast and adapt to these extreme events. It is expected that more severe droughts, larger precipitation events, and more frequent anomalous wet and dry spells will become the "new normal" for many ecosystems (Lewis et al. 2017; Seneviratne et al. 2021). Further compounding (concurrent or

Communicated by George Zittis

✉ Rubina Ansari
r.ansari@unibs.it

Ana Casanueva
ana.casanueva@unican.es

Muhammad Usman Liaqat
usmanliaqat0321@gmail.com

Giovanna Grossi
giovanna.grossi@unibs.it

[1] Department of Civil, Environmental, Architectural Engineering and Mathematics, University of Brescia, Via Branze 43, Brescia, Italy

[2] Deptartment of Irrigation and Drainage, University of Agriculture Faisalabad, Canal Road, Faisalabad, Pakistan

[3] Dept. Matemática Aplicada y Ciencias de La Computación (MACC), Universidad de Cantabria, Avda. Los Castros s/n, Santander, Spain

[4] Grupo de Meteorología y Computación, Universidad de Cantabria (Unidad Asociada al CSIC), Avda. Los Castros s/n, Santander, Spain

consecutive occurrences of multiple weather and climate drivers) of these extreme events across space or/and time may provoke greater impacts than what would have been caused by a single event, even when the individual contributing variables are not extreme (Zscheischler et al. 2020). These extreme events have put a strain on society's ability to predict and adapt effectively to these extreme phenomena.

The most important and commonly studied compound events in hydro-climatology are those associated with precipitation and temperature. The occurrence of compound events can be attributed to various factors, including external influences (e.g., changes in regional warming), allied strengthening of multiple extremes (e.g., land surface feedback), or conditional dependence (e.g., interplay between antecedent soil moisture levels and preceding precipitation in triggering floods and droughts).

The definition and classification of compound events have garnered notable consideration over the past few decades. To aid the framing and development of new research on compound events, Zscheischler et al. (2020) proposed four distinct classes of compound events and their different physical characteristics (modulators, drivers, hazards, and impacts) that form a compound event. Such events can occur in multiple ways due to the complex nature of the climate system, for example, "Preconditioned" events, where pre-existing weather or climate conditions can intensify the impact of hazard; "Multivariate" events, where the simultaneous occurrences of multiple drivers and/or hazards at the same location result in greater impacts; "Temporal compound" events, where impacts are due to the consecutive occurrences of multiple hazards within a particular geographical region, and "Spatially compound" events, where synchronized occurrences of individual hazards across multiple regions lead to an impact.

Compound events drivers and their additive impacts on regional and global scales have been the subject of several studies. For instance, the combinations of quasi-synchronous extremes across multiple regions can lead to amplifying effects on connected global systems (Raymond et al. 2020). A severe drought that occurred concurrently in Asia, Brazil, and Africa during 1876–1878 resulted in synchronous crop failures in these regions, posing a threat to food security (Singh et al. 2018). Other studies have examined the increased probability of concurrent heatwaves and regional droughts with changes in large-scale circulation modes under warming scenarios (Kornhuber et al. 2020; Singh et al. 2022) and the following synchronized crop failures across major breadbasket regions of the world (Anderson et al. 2019; Gaupp et al. 2020).

Temporal compound events (TCEs) can be of the same type, such as multiple consecutive heatwaves (Baldwin et al. 2019), droughts (Bastos et al. 2021; van der Wiel et al. 2023), or consecutive heavy precipitation events (Fish et al. 2022; Kopp et al. 2021), or different hazards, for example, simultaneous occurrence of heavy precipitation and wind extremes (Messmer and Simmonds 2021; Owen et al. 2021), compound flooding in coastal areas as a result of simultaneous occurrence of storm surge and heavy precipitation (Ridder et al. 2018; Zellou and Rahali 2019), a flood event at the end of heatwave or drought (He and Sheffield 2020; Zhang et al. 2021), simultaneous drought and heatwave (Sutanto et al. 2020; Zscheischler and Fischer 2020), rain-on-snow flood events due to concurrent occurrence of heavy precipitation and snowmelt (Li et al. 2019; López-Moreno et al. 2021), or epidemics followed by floods (Donges et al. 2016).

A quantification of the TCEs is imperative for assessing the risk of associated potential impacts, both in past and future climate scenarios. A number of above studies have focused primarily on the concurrent occurrence of compound events, but a limited number have examined the consecutive occurrence of contrasting hydrological extremes (i.e., wet and dry extreme events). It has been observed that an increase in floods is normally accompanied by a decrease in droughts due to more rainfall. Conversely, a reduced rainfall is typically associated with an increase in droughts (Gudmundsson et al. 2021). However, some models project that both the frequency and severity of hydrological extremes may increase simultaneously, a phenomenon known as acceleration of the terrestrial component of the hydrological cycle (Kreibich et al. 2022).

In this context, we have specifically considered TCEs for a situation where two contrasting extremes, namely wet and dry events, occur consecutively at the same location (as a subset of the broader compound events definition). The consecutive occurrence of these extreme events can exacerbate adverse impacts resulting from individual hazards alone, as recently witnessed in Pakistan, 2022 (Wang et al. 2023), Queensland-Australia, 2010 (Beard et al. 2011), UK, 2012 (Parry et al. 2013), India, 2016 (Roxy et al. 2017), and Japan, 2018 (Wang et al. 2019). The effects of compound wet and dry extreme events have also been studied under current and warming climate conditions. For instance, Visser-Quinn et al. (2019) and Zhao et al. (2020) identified geographical hotspots for spatio-temporally concurrent floods and droughts in the UK and Hanjiang River Basin, China, respectively. Other examples include the analysis of rapid transitions of wet-dry extreme events in mainland China (Qiao et al. 2022), in Upper Jhelum Basin-Pakistan (Ansari and Grossi 2022), and in southeast Australia (Holgate et al. 2023).

In general, the impacts of temporal compounding of wet and dry events seem to be mostly related to rapid changes in vulnerability. A dry event may cause increases in the vulnerability of people, crops, or livestock, which causes impacts of a subsequent or co-occurring wet event to be worse than

from a wet event that is not preceded by a dry event. This depends on initial vulnerability and the speed of community recovery, as impacts and change in vulnerability vary across different groups. In the agriculture and livestock sector, the additive impacts of such temporal compound events, especially in low- and lower-middle-income countries, often worsen outcomes. For example, droughts can weaken livestock, increasing vulnerability to subsequent floods, as seen in Queensland in 2019 when many cattle died (Cowan et al. 2022). Vegetation and crop yield are also affected by consecutive dry-to-wet events, impacting crop size and yield based on soil and growth stages (Gao et al. 2019; McCarthy et al. 2021). Furthermore, these events degrade water quality and foster conditions for disease. Pollutants accumulated during dry periods are washed into rivers during floods, raising phosphorus levels and potentially causing fish mortality and water eutrophication (Laudon et al. 2005; Mishra et al. 2021; Wurtsbaugh et al. 2019).

It is therefore important to analyze the temporal compounding of extreme wet and dry events in a changing environment to comprehensively assess their consequences on water-dependent sectors and develop effective adaptation strategies, including the development of improved reservoir operation protocols and agricultural planning.

The present study builds upon Ansari et al. (2023), which shows a comprehensive present-climate evaluation of raw and bias-corrected climate model simulations regarding the temporal aspects and multivariate dependency of essential climatic variables, and main characteristics of moderate to extreme wet and dry events in the UJB. The UJB is located at the foothills of Western Himalaya, one of the mountainous ranges most affected by climate change. The region has already witnessed an increase in extreme hydro-meteorological events in the last few decades (Pachauri et al. 2014), and hence, the projection of these events cannot be left apart in the development of the climate change adaptation strategy for the region. Here, we examine the projected changes in moderate to extreme wet and dry events and their compounding in temporal dimension over UJB using climate models output from three modeling experiments (CMIP6, CORDEX, and CORDEX-CORE), bias corrected with three different BC methods under low, medium, and high emission scenarios for two future periods (2040–2059 and 2080–2099). Specifically, the present study aims to examine:

- The projected changes in the characteristics of wet and dry events (i.e., duration, severity, and frequency) and in the probability of TCEs.
- The uncertainty associated with different bias correction (BC) methods and approaches in the climate change signal of such events characteristics and TCEs.

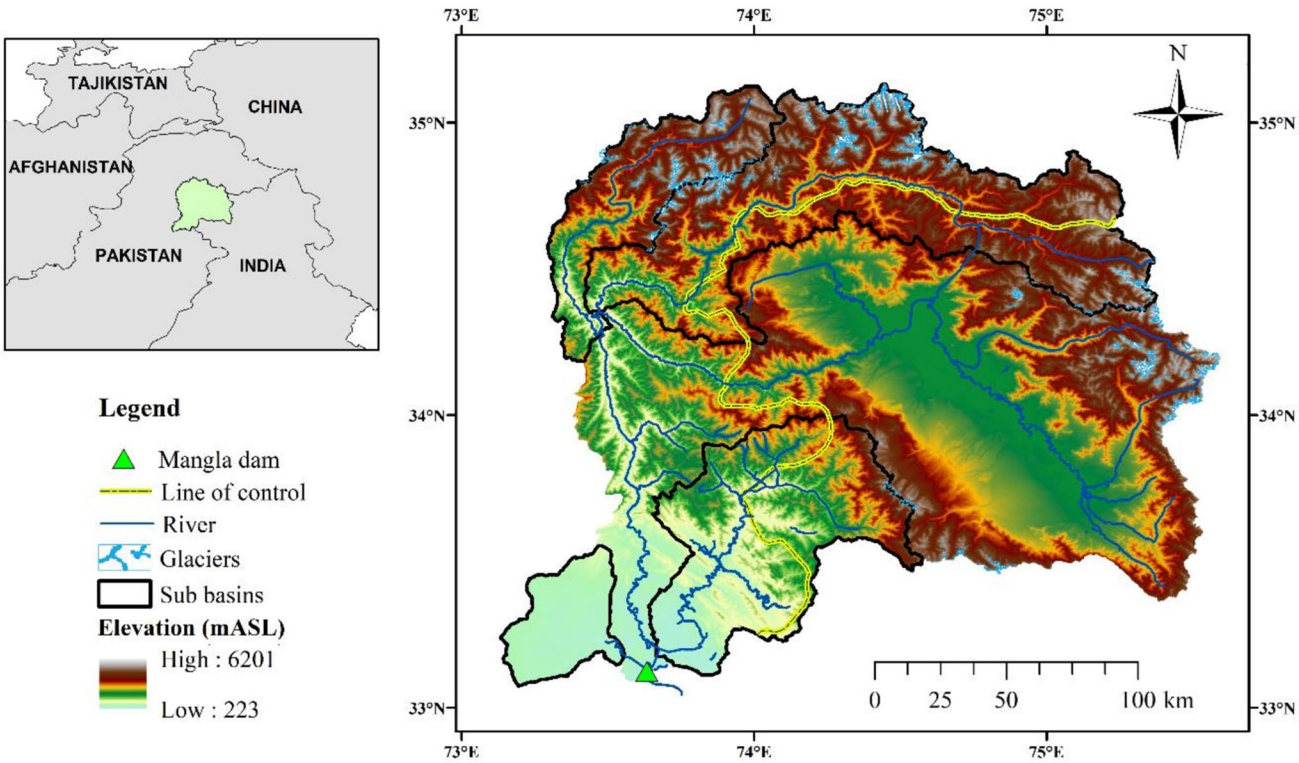

Fig. 1 Geographical location and topography of the Upper Jhelum basin, along with location of sub-basins (black polygons), Mangla dam (filled green triangle), glaciers (filled white polygons with blue boundaries), and the line of control (yellow highlighted dashed line)

Characteristics of the study area

The proposed framework is implemented in the source region of the Jhelum River, known as the Upper Jhelum Basin (UJB), which is geographically located between latitudes 33°00′ N and 35°12′ N, and longitudes 73°07′ E and 75°40′ E (Fig. 1). The basin drains the foothills of the western Himalaya and Pir-Panjal mountains and feeds the second largest reservoir of Pakistan, the "Mangla Reservoir." The landscape of the basin is characterized by extreme topographical variations, 223–6201 m above sea level (masl) within a 33,467 km^2 expanse. Approximately 73% (24,431 km^2) of the UJB area lies below its mean elevation (2353 masl). Approximately 0.75% (252 km^2) of the basin is covered by perennial glaciers in the north of the basin (Consortium and Inventory 2017). Grass, forest, and agriculture are the three major land use–land cover types dominating over high-, mid-, and low-elevation areas respectively. Permanent snow and ice cover a negligible area in the northwest of the basin, whereas a small patch of barren land exists over the densely grassy mountains of the western Himalaya and Pir Panjal. The urban settlement covers a small portion of the basin, concentrated in the Kashmir valley (Ansari et al. 2024).

The hydro-climatology in the UJB is characterized by two distinct precipitation regimes: Indian Summer Monsoon and westerlies. The effect and contribution of both precipitation regimes vary spatially, as well as temporally (Ul Hasson et al. 2016). The monsoon precipitation system brings precipitation as rain and is dominant in southern parts of the basin. The strength of the Monsoon system decreases progressively northward towards the foothills of the Western Himalayas, where the influence of westerlies is more pronounced (Archer and Fowler 2008) which brings precipitation as snow. The basin average annual precipitation and temperature are about 1150 mm $year^{-1}$ and 13.2 °C, respectively (Ansari and Grossi 2022).

Data and methods

Definition of extreme wet-dry events and their characteristics

A multivariate drought index named SPEI (Vicente-Serrano et al. 2010) is utilized to define wet and dry events. The SPEI is computed using a 30-day accumulation period of climatic water balance (precipitation minus potential evapotranspiration) at a daily time step. The potential evapotranspiration is calculated using the Hargreaves-Samani method (Hargreaves and Samani 1985) based on daily maximum and minimum temperature. The extraterrestrial radiation required in this method is computed based on the latitude of each grid cell and the day of the year. For detailed procedure and equations for the SPEI calculations, readers are encouraged to refer to the studies by Vicente-Serrano et al. (2010) and Ansari et al. (2023).

Monthly SPEI series (aggregation of daily SPEI series) is used to identify moderate to extreme wet and dry events as positive ($SPEI \geq 1$) and negative ($SPEI \leq -1$) values that persist for a minimum of 2 months consecutively, respectively. These choices about accumulation period, monthly time series, and minimum length of events are motivated by our focus on floods and short-term droughts. Such events are not clearly associated with long-term SPEI due to the averaging effect of accumulated precipitation and temperature over extended periods, which can overshadow the signals of extreme precipitation and temperature events occurring over shorter durations. Our approach allows for a more accurate identification of wet and dry events, which serve as the primary drivers of hydrological floods and droughts. The thresholds used to define these extreme events are commonly employed in previous research works (Svoboda et al. 2012). Although this SPEI threshold (± 1) is used to define moderate wet and dry events, which may not have extreme impacts when they occur individually, their combined impact can be more severe than the sum of their individual effects. For instance, a dry event can increase the vulnerability of people, crops, or livestock, making the consequences of a subsequent or co-occurring wet event worse than if the wet event had occurred on its own. Additionally, this threshold captures events ranging from moderate to severe and extreme, ensuring sufficient sampling of events during the study period for further analysis. Duration, severity, and absolute frequency are used to characterize these wet and dry events. The duration of wet (WD) and dry (DD) events is defined as the length of time (months) in which the SPEI value is consecutively above 1 or below -1, respectively. The severity of wet (WS) and dry (DS) events is the cumulative value of the SPEI during the whole duration of the event. The absolute frequency of wet (WF) and dry (DF) events is the total number of occurrences in a given time frame. As both duration and severity are calculated for each event, the median value across all the identified events is considered a single index.

Temporally compound events and event coincidence analysis

TCEs, which are defined as consecutive occurrence of two contrary powerful states (here wet and dry events) in the adjacent months, include D-to-W events and W-to-D events. Hence, the minimum duration of a TCE is 2 months. D-to-W TCE is defined as a dry event ($SPEI_i \leq -1$) suddenly terminated by a wet event ($SPEI_{i+1} \geq 1$) in the following month.

On the other hand, a W-to-D TCE is defined as a wet event ($SPEI_i \geq 1$) abruptly changes into a dry event ($SPEI_{i+1} \leq -1$) in the subsequent month.

To investigate the statistical interdependence of wet-dry events and their significance, the present study employs Event Coincidence Analysis (ECA, Donges et al. (2016)). ECA is a novel statistical method that enables the characterization of lagged and time-varying relationships between two events by using a time lag parameter (τ) within a temporal tolerance window (ΔT). The trigger coincidence rate (r) for both types of TCEs is calculated as:

$$r^{D \Rightarrow W}(\Delta T, \tau) = \frac{1}{N_D} \sum_{j=1}^{N_D} \Theta \left[\sum_{i=1}^{N_W} 1_{[0,\Delta T]} \left(\left(t_i^W - \tau \right) - t_j^D \right) \right]$$

$$r^{W \Rightarrow D}(\Delta T, \tau) = \frac{1}{N_W} \sum_{j=1}^{N_W} \Theta \left[\sum_{i=1}^{N_D} 1_{[0,\Delta T]} \left(\left(t_i^D - \tau \right) - t_j^W \right) \right]$$

where Θ is the Heaviside function

$$\Theta(x) := \begin{cases} 1 \; x > 0 \\ 0 \; x \leq 0 \end{cases}$$

and $1_{[0,\Delta T]}(\cdot)$ is the indicator function of the specified time window $[0,\Delta T]$:

$$1_{[0,\Delta T]}(x) := \begin{cases} 1 \; if \; x \in [0, \Delta T] \\ 0 \; if \; x \notin [0, \Delta T] \end{cases}$$

N_W and N_D denote the total number of wet and dry events with their timing of the event t_i^W and t_i^D respectively. Here, we choose $\tau = 1$, as this represents the rapid transition of two contrasting events in adjacent months. In addition, an analytical significance test (p-value < 0.05) is carried out to evaluate the robustness of the statistical relationship between wet and dry events with the null hypothesis that the consecutive occurrence of wet and dry events is randomly distributed as the result of Poisson processes.

Climate models output and bias correction

In the present study, we use all available Regional Climate Models (RCM) output of the CORDEX and CORDEX-CORE initiative for the south Asian domain (denoted as WAS) under all available emission scenarios (i.e., representative concentration pathways (RCPs)). These simulations were produced by dynamically downscaling the CMIP5 Global Climate Models (GCMs), with a horizontal spatial resolution of 0.44° and 0.22° on rotated grids (approximately 50 km and 25 km), respectively (Giorgi et al. 2009; Jones 2010; Teichmann et al. 2021). Additionally, 2 GCMs of the CMIP6 experiment are also considered that are available at a similar resolution to the CORDEX simulations (Eyring et al. 2015). The emission scenarios used in the CMIP6 experiment are shared socio-economic pathways (SSPs) which are different from CORDEX and CORDEX-CORE RCMs, simulations as these RCM simulations are driven by CMIP5 models. RCPs and SSPs provide different scenarios including different evolutions of greenhouse gas (GHG) emissions, climate policies, and socio-economic development. While RCPs focus purely on radiative forcing and GHG emissions, SSPs provide a more holistic view of possible futures, incorporating socio-economic conditions like population growth, economic development, and the effectiveness of climate policies. Although there are some differences between SSPs and RCPs, the chosen emission scenarios approximate the same level of aggregated radiative forcing (Tebaldi et al. 2021). The emission scenarios (RCP2.6/SSP126, RCP4.5/SSP545, and RCP8.5/SSP585) range from a mitigation scenario involving rapid and substantial reductions in global greenhouse gas emissions, with global temperature rise limited to approximately 1.5–2 °C (RCP2.6/SSP126), to a high emission scenario where emissions continue to grow, leading to a temperature increase exceeding 4 °C (RCP8.5/SSP585) by the end of the century (O'Neill et al. 2014; Van Vuuren et al. 2011). In total, the present study utilized 28 climate model simulations. Figure 2 presents the climate models and scenarios employed in this study. For detailed description of the used climate models, their spatial resolution, contributing modeling center, and driving GCM can be found in Ansari et al. (2023).

Climate models are the main tool to project future climate. Nevertheless, these models are often subject to systematic biases resulting from inaccurate representation of physical processes. BC is typically applied as a post processing step to overcome this issue, especially for threshold-based derived indices. The present study employed two univariate (Empirical Quantile Mapping (EQM) and Quantile Delta Mapping (QDM)) and one multivariate (Multivariate Bias Correction with N-dimensional probability density function transform (MBCn)) BC methods to reduce the biases in climate model simulations, using W5E5 as reference dataset. The W5E5 is a global dataset with spatial resolution of 0.5° at daily time step for a period of 1979–2016. This dataset was developed by combining the WATer and global CHange (WATCH) Forcing Data methodology applied to ERA5 reanalysis data (WFDE5) v1.0 (Cucchi et al. 2020; Weedon et al. 2014) over land with ERA5 (Hersbach et al. 2020) over the ocean. EQM is an empirical method, in which a transfer function is calibrated on the training period to align all quantiles of the model empirical distribution with the corresponding reference distribution (Déqué 2007). Out-of-sample values are adjusted through constant extrapolation. Additionally, the adjusted wet-day threshold and frequency adaptation techniques suggested by Themeßl et al.

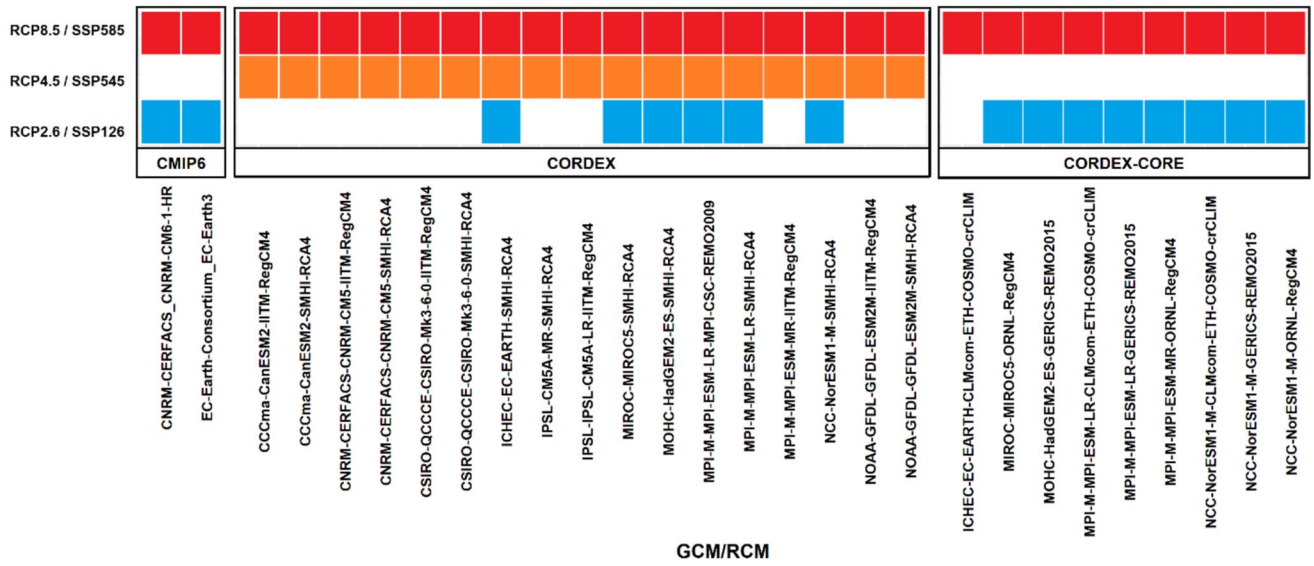

Fig. 2 Climate model simulations and emission scenarios used in the present study

(2012) and Wilcke et al. (2013) are used to adjust the model's overestimation of the frequency of wet and dry days, respectively. QDM is a trend-preserving empirical method, consists of three steps: (i) trends removal from each quantile of the model projections, (ii) application of empirical quantile mapping to the detrended series, and (iii) addition of the removed projected future trends to the bias-corrected quantiles (Cannon et al. 2015). The MBCn method not only adjusts the individual univariate features of each variable but also their multivariate interdependence simultaneously. It uses randomly generated orthogonal matrices to partially decorrelate the climate variables prior to QDM application on each of variables separately to adjust the marginal distributions. The process is repeated iteratively until the model data distribution converges to that of the reference data distribution (Cannon 2018). This convergence is verified on the basis of the energy distance score (Rizzo and Székely 2016).

The univariate BC methods are employed through two different approaches: (1) the component-wise approach (CW), in which each climatic variable involved in SPEI calculation is individually subjected to the BC, and (2) the direct approach (D), in which the uncorrected SPEI is directly subjected to BC. All BC methods are calibrated in the historical period (1986–2005) and applied in two future periods (2040–2059 and 2080–2099). All considered BC methods presume that the biases present in climate model simulations are constant over time and apply the same calibrated transfer function to the projected climate, which could result in modification of the original model change signals for non-trend-preserving BC methods (here EQM). The selection of these BC methods is based on Ansari et al. (2023) which evaluate the performance of various BC methods (uni- and multivariate) and BC approaches (direct and component-wise) in terms of univariate indices related to temporal aspects of the essential climate variables used for SPEI calculation, their multivariate dependency, and biases in the SPEI-derived indices during the historical period (1986–2005).

Results

Future changes in Standardized Precipitation Evapotranspiration Index indices

The spatial distribution of climate change signals of SPEI indices relative to the baseline period (1986–2005), for the multi-model raw and bias-corrected ensembles, separately for CMIP6 (2 simulations), CORDEX (17 simulations), and CORDEX-CORE (9 simulations) are shown in Figs. S1–S6. The climate change signals are calculated for the near (2040–2059) and far (2080–2099) future periods under low, medium, and high emission scenarios. Results show contrasting climate change signals for both BC approaches with the direct correction introducing a larger modification of the original (raw) change signals especially for severity and frequency indices. This modification by the direct approach is usually towards positive change

signals. Further, given a particular approach, BC methods present similar climate change signals regardless of SPEI indices, emission scenarios, and time period.

Regarding climate model experiments, CORDEX and CORDEX-CORE (WAS44 and WAS22, respectively) ensemble present opposite sign climate change signals for duration indices (duration of dry and wet events) with no specific spatial pattern whereas the change signals from CMIP6 ensemble divide the region into two distinct parts, i.e., northeast (which host foothills of western Himalaya) and southwest (relatively plain region with dominance of monsoon precipitation system). These results regarding the spatial patterns hold for most of the SPEI indices, emission scenarios, and time segments. For instance, dry event indices (i.e., duration, severity, and frequency of dry events) and frequency of wet events show negative and positive climate change signals in northeast and southwest regions, respectively, under high emission scenarios. Differences between the different ensembles also exist for the spatial distribution of the changes in severity indices (severity of dry and wet events). For instance, under the high emission scenarios, the CMIP6 ensemble projected an increase in the severity of wet events over most parts of the basin and mixed signals are found for the severity of dry events. Conversely, WAS44 and WAS22 ensembles projected an increase in the severity of dry events over the whole basin and mixed change signals for wet ones.

The climate change signals for regionally averaged SPEI indices for all individual climate simulations are summarized in Figs. 3 and 4. Overall, climate models from all considered experiments present larger spread for wet indices compared to dry indices. The spread is usually determined by WAS-44 climate models for most of the SPEI indices under considered BC methods, time segments, and emission scenarios which could be due to the largest number of simulations. However, there are exceptions for CMIP6 and WAS-22, especially for the duration and severity indices (particularly for the duration and severity of dry events, DD and DS) under different BC methods. The reduction in model spread is evident after BC under the component-wise approach and the multivariate method, whereas the modification of the signals by the direct approach leads to a slight increase in climate model spread. These findings are consistent with all considered time periods and emission scenarios.

Temporal compound events

Next, we examine the spatial distribution of probability of temporally compound events (D-to-W and W-to-D, see the "Data and methods" section) and their statistical significance for the historical (according to W5E5) and projected future climate, for the raw and bias-corrected climate models output for the near (2040–2059) and far (2080–2099) future periods under low (RCP26/SSP1–2.6), moderate (RCP45/SSP2–4.5), and high (RCP85/SSP5–8.5) emission scenarios.

Figure 5 shows that the probability of D-to-W TCEs is particularly high (reaching up to 60%) in southwest of the basin, a monsoon-dominated region, and statistically significant over 23.33% of the domain (with p-value less than 0.05). On the other hand, non-statistically significant results (at the 5% significance level) are observed for W-to-D TCEs, without any discernible pattern of occurrence during the historical period (Fig. S7). Interestingly, the southwest of the basin, which is not a hotspot for either dry or wet events separately (Ansari et al. 2023), exhibits a high probability (up to 60%) of D-to-W TCEs during the historical period, i.e., of enhanced compound events. The northeast part of the basin, which host foothills of western Himalayas (under westerlies precipitation pattern), is found to be least effected by TCEs despite its higher susceptibility towards wet and dry moderate to extreme events, characterized by higher severity and duration (Ansari et al. 2023).

Regarding future projections, the spatial patterns of projected probability of TCEs are consistent with those of the historical period, revealing the southwest part of the basin as a hotspot for D-to-W TCEs. However, there are some discrepancies among the climate model ensembles. CORDEX ensembles (WAS-44 and WAS-22) indicate a slight decrease in the probability of D-to-W TCEs by the end of the century particularly under the lowest emission scenario, whereas the CMIP6 ensemble shows an increase in probability of D-to-W TCEs by the end of century under all emission scenarios and time periods. Further, the probabilities of D-to-W TCEs are found to be statistically significant with medium to high models' agreement (i.e., number of models agreeing on the statistical significance of the TCEs).

The three raw climate model ensembles show decreasing probabilities of D-to-W TCEs relative to the baseline period under all emission scenarios and time segments. This is especially true for CORDEX and CORDEX-CORE ensembles with also lower models' agreement in terms of statistically significant probabilities. Conversely, the southwest of the basin is a hotspot for the D-to-W TCEs for the raw CMIP6 ensemble with medium models' agreement. Overall, none of the BC methods under both approaches preserves the raw climate change signals except for CMIP6 ensemble which show a slight preservation of raw climate change signals in terms of spatial patterns. In general, BC modifies the probabilities of the raw models by increasing the probability of D-to-W TCEs and model agreement, for both future periods and all emission scenarios. Similar to SPEI indices, the BC methods under the direct approach (i.e., D-EQM and D-QDM) present similar climate change signals whereas the climate change signals projected by MBCn are somewhat

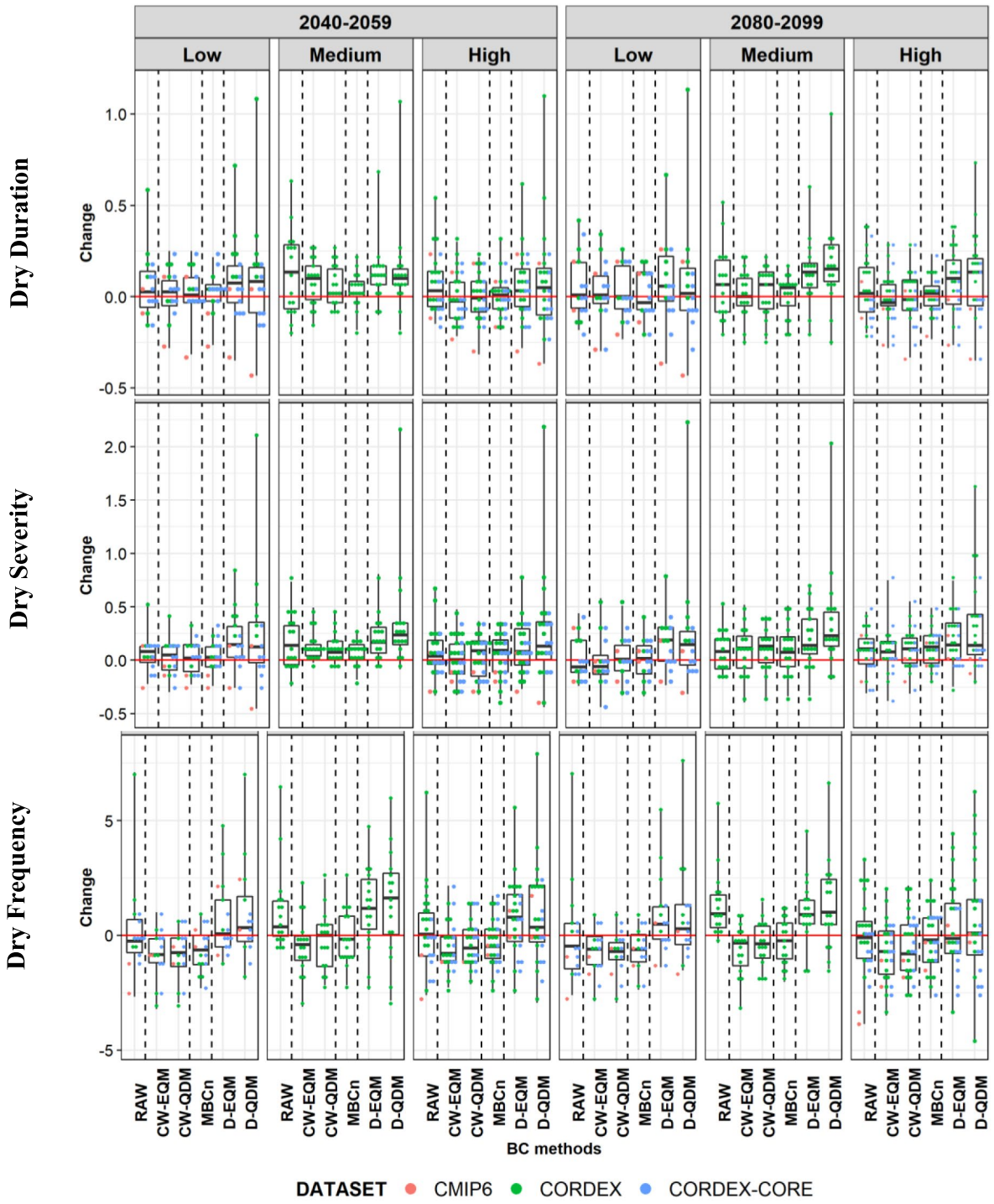

Fig. 3 Absolute climate change signals of spatially averaged SPEI-derived dry indices (duration: upper row; severity: middle row; frequency: lower row) over the Upper Jhelum Basin for the near future (2040–2059) and far future (2080–2099) with respect to baseline period (1986–2005) under low (RCP2.6/SSP126), medium (RCP4.5/SSP545), and high (RCP8.5/SSP585) emission scenarios. The indices are calculated from both raw and bias-corrected climate model output, with individual model results depicted in colored dots (CMIP6 in red, CORDEX in green, CORDEX-CORE in blue) within each box, which indicates the interquartile model spread. The whiskers extend to the full range of change signals, while the red horizontal lines indicate no change from the baseline period

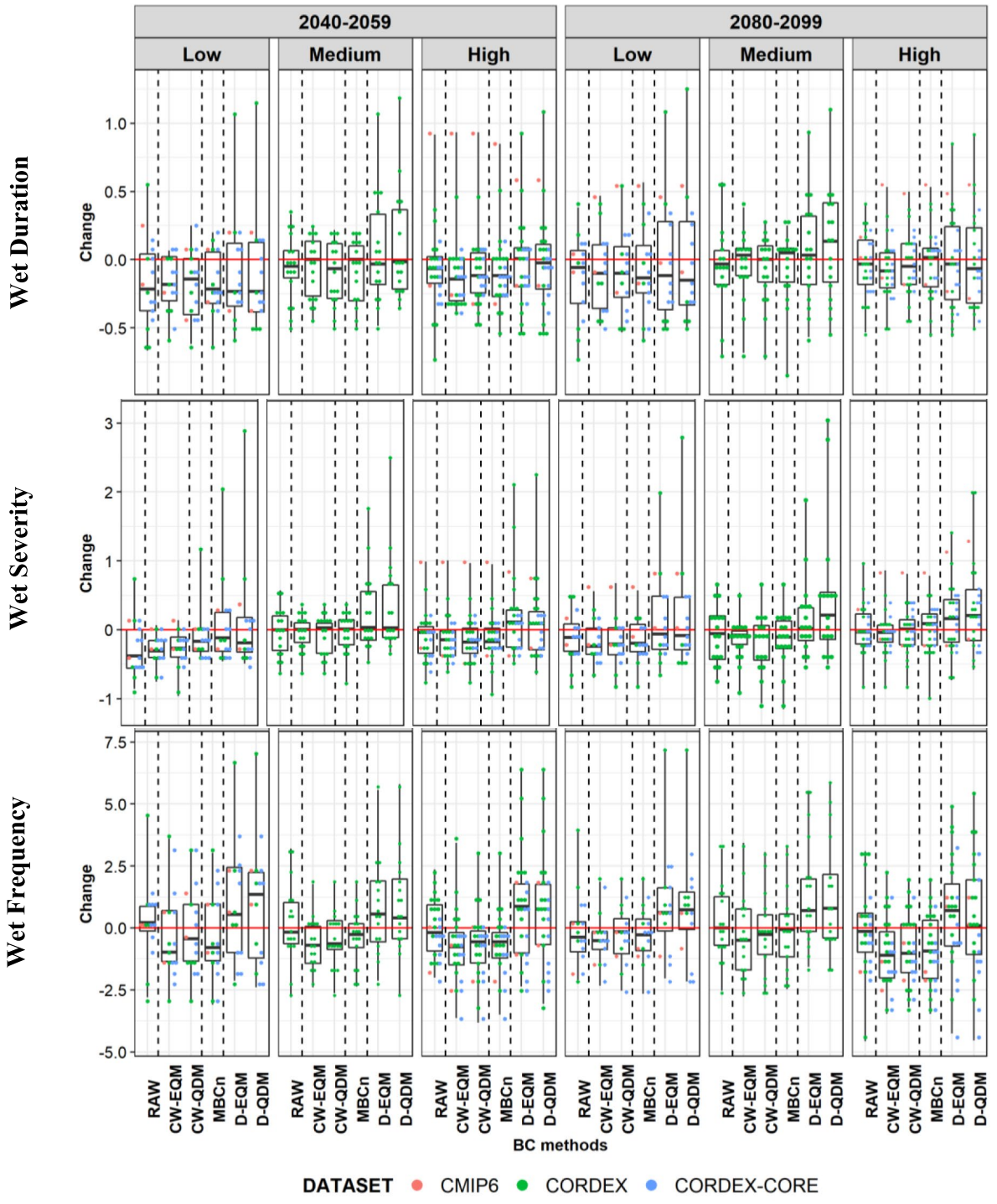

Fig. 4 Same as Fig. 2 but for SPEI-derived wet indices

similar to those projected by BC methods under the component-wise approach (i.e., CW-EQM and CW-QDM).

The climate change signals for the regionally averaged probabilities of D-to-W TCEs for each individual climate simulation are depicted in Fig. 6. Similar to SPEI indices, a reduction in model spread is found after BC under the component-wise approach and the multivariate method, whereas the direct approach increases climate model spread by increasing the probability of TCEs. These findings are consistent for all considered time periods and emission scenarios.

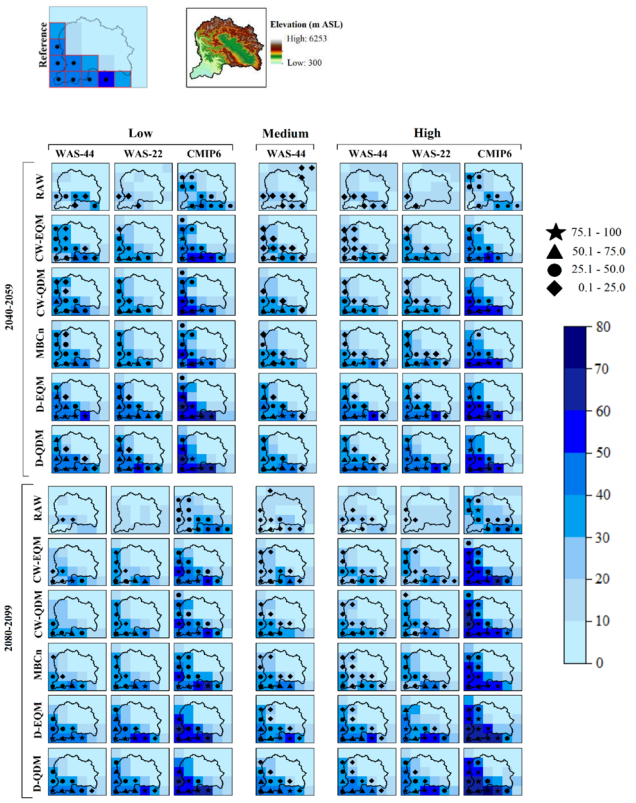

Fig. 5 Probability of temporal compound dry-to-wet events (%), in the historical reference dataset (1986–2005, first row, left), alongside the digital elevation model of the area in meters above sea level (first row, right) and future projected probabilities for the near future (2040–2059) and far future (2080–2099) under low (RCP2.6/SSP126), medium (RCP4.5/SSP545), and high (RCP8.5/SSP585) emission scenarios. These projections are based on the multi-model ensemble mean raw ensembles (second row) and bias-corrected ensembles, for two bias correction approaches and three bias correction methods (rest of the rows). In the projections, the different shapes denote the percentage of ensemble members with statistically significant probability at the 5% level. The highlighted grid boxes in the first row are utilized for further analyses in Fig. 6

Discussion and conclusions

This study examines future climate projections for extreme wet-dry events, as well as their temporal compounding using climate models output from three modeling experiments (CMIP6, CORDEX, and CORDEX-CORE) bias corrected by two univariate BC methods (i.e., EQM and QDM) under two bias correction approaches (component-wise-CW and direct-D) and a multivariate BC method (N-dimensions-MBCn). The wet and dry events are characterized using SPEI-derived indices (namely duration, severity, and frequency) and climate change signals are estimated for the near future (2040–2059) and far future (2080–2099) with respect to the baseline period (1986–2005). The present study also focuses on temporal compounding of these contrasting events, both in historical future climate contexts, as the consecutive occurrence of wet and dry events challenges water resources management and can be particularly impactful.

Future projections of the individual wet and dry extreme events (in terms of duration, severity, frequency) show varying climate change signals for all SPEI indices under all considered BC methods, BC approaches, emission scenarios, and time segments. Specifically, the frequency and severity of wet and dry events are projected to increase, which is expected under warming conditions and was reported by previous literature. For instance, Panday et al. (2015) and Sanjay et al. (2017) reported that there will be a rise in the frequency and intensity of extreme rainfall events across the Himalayan–Tibetan Plateau mountains during the twenty-first century, especially during the monsoon season. Another study indicates that droughts are expected to be more frequent, severe, and widespread over the mainland India during the latter half of the twenty-first century, while increase in flood events are projected for the major Himalayan River basins such as Indus, Ganga, and Brahmaputra (Mujumdar et al. 2020).

Regarding TCEs, the observed probabilities of dry-to-wet (D-to-W) and wet-to-dry (W-to-D) TCEs are found to be high up to 60% and 30%, respectively. The probability of D-to-W TCEs is projected to increase from 60 to 80% (for specific grid boxes and model simulations) whereas the probability of W-to-D TCEs approximately remains unchanged under warming conditions. This low to moderate increment in the D-to-W TCEs under anticipated future conditions is in agreement with Gu et al. (2022), who found a clearer increment in the fraction of TCEs (number of TCEs to total flood events) in the tropical regions, followed by arid, temperate, cold regions, and polar zone (note that low- and high-altitude areas of UJB lie in the temperate and polar climate regions, respectively). Conversely, Zhang et al.(2021) found a decrease in the probability of such TCEs in the tropics albeit with increased frequency of heavy rainfall events. A global study conducted by Zhang et al. (2021) highlighted the spatial hotspots for the compound drought and extreme rainfall events under a warming world. According to that study, 66% of CMIP5 models showed a decreased future probability of such TCEs in the second half of the century (2051–2100) over the southern Asia (SAS) under the worst-case scenario, i.e., RCP8.5. Another global study found a historical (1950–2016) probability of 21.6% and 20.7% for drought-pluvial seesaw with 3-month lag period over SAS for the boreal spring–summer and fall-winter, respectively (He and Sheffield 2020). The differences among these studies could be due to the varying methodological framework, such as the threshold to define wet and dry extreme events (e.g., low vs. high), the choice of the index (e.g., variables involved in the calculation of the index and their

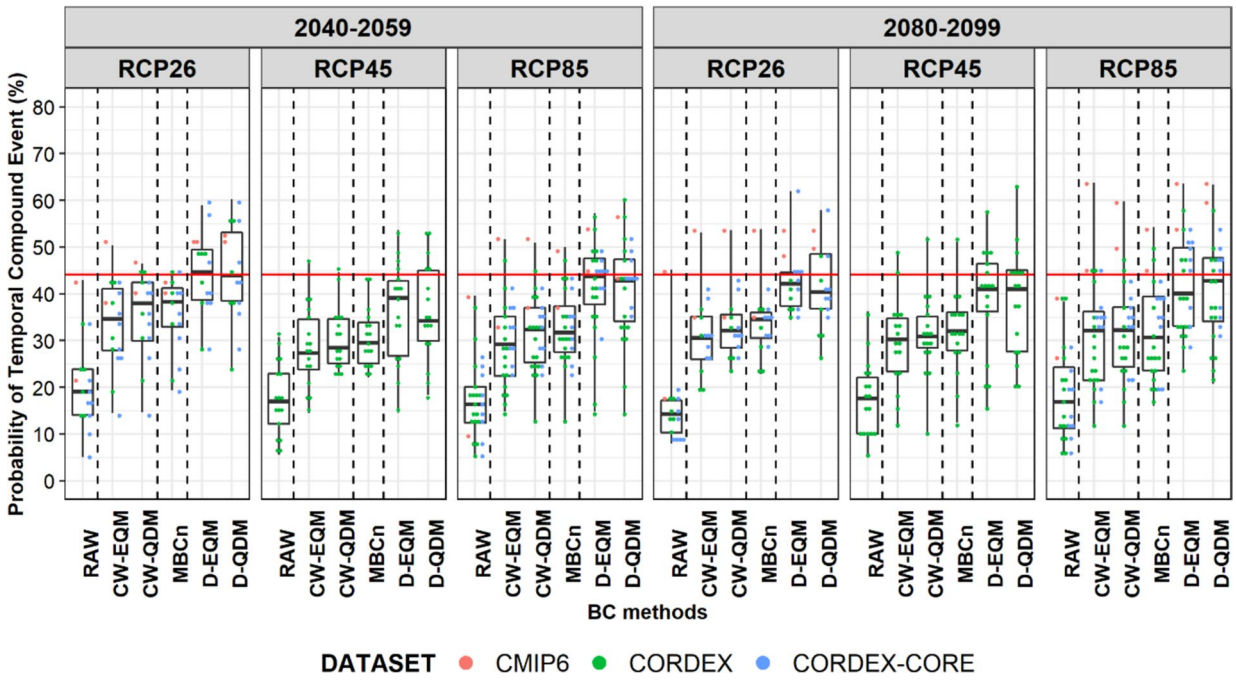

Fig. 6 Probability of temporal compound dry-to-wet events (%), spatially averaged over ten grid boxes highlighted in Fig. 5, for the near future (2040–2059) and far future (2080–2099) under low (RCP2.6/SSP126), medium (RCP4.5/SSP545), and high (RCP8.5/SSP585) emission scenarios. The probabilities are calculated from the raw (first box in each panel) and bias corrected climate model output (remaining boxes), with individual model results depicted in colored dots (CMIP6 in red, CORDEX in green, CORDEX-CORE in blue) within each box. Each box indicates the interquartile model spread and whiskers expand to the full range of probability of temporal compound event. Red horizontal lines depict the probability of temporal compound events in the baseline period (1986–2005) according to the observations

interdependency), the lag time (which indicates the rapidness of event alteration), and the temporal window interval (which indicates the uncertain onset of extreme events). Due to the distinct methodological frameworks employed in each study, which are tailored to specific sectors and objectives, direct comparisons between the outcomes of this research and those of previous studies cannot be made. Nonetheless, our findings are consistent with the overall conclusions of these earlier studies, demonstrating that dry events are frequently associated with a rise in subsequent extreme wet events.

In terms of spatial extent, in the present work, about 23% of the total study region has experienced statistically significant ($p < 0.05$) probability of D-to-W TCEs during the historical period and it is projected to increase for most of the considered datasets, emission scenarios, and time segments after BC. Although D-to-W TCEs affect the small proportion of the basin, we identify the spatial hotspots, located in the southwest of the basin where precipitation is dominated by the monsoon system, which was not found to be a hotspot neither for dry nor for wet events separately (Ansari et al. 2023). Although the seasonality of TCEs is beyond the scope of the current study, it is more likely that the D-to-W TCEs will occur during summer season because the hotspot region usually receives heavy precipitation during summer season under monsoon system (Ansari et al. 2022; Archer and Fowler 2008; Azmat 2015; Mahmood 2013). Depending on the BC method, datasets, emission scenarios, and time segments, a negligible to large increase in most of the (individual) wet and dry events indices is expected in this hotspot in the anticipated future. Particularly, the CMIP6 ensemble presents strong climate change signals (either positive or negative) under the strong emission scenario with a clear pattern of occurrence and the southwest of the basin stands out as a hotspot for the more frequent wet and dry extreme events with an increase in frequency of wet and dry events up to eight events relative to the baseline period, respectively. In contrast, the northeast part of the basin which hosts foothills of western Himalayas (under westerlies precipitation pattern) is found to be less affected by TCEs despite its higher susceptibility towards wet and dry events with higher severity and duration during the historical period (Ansari et al. 2023). The increase in TCEs may also become apparent in areas with projected decline in the extreme dry and/or wet events (Gu et al. 2022; Zhang et al. 2021). For instance, Zhang et al. (2021) found that 27 – 41% of the global land area in Northern China and Southern Africa is expected to encounter less drought events but experience high

probabilities of successive drought-flood events. In contrast, 4 – 13% of the world's landmass, including regions such as Southern Africa, Australia, Northern Mexico, southwestern US, and Southwest coast of South America, are expected to suffer from higher probability of droughts followed by floods but a lower frequency of heavy rainfall, which shows that heavy rainfall is likely to be more frequent at the drought termination, despite a decrease in the overall frequency of heavy rainfall events.

In contrast to D-to-W TCEs, the W-to-D TCEs are found to be less apparent without specific pattern of occurrence in the historical period as well as in future climate conditions, in line with previous studies (e.g., Qiao et al. (2022) in China).

Explaining the patterns of TCEs from a physical perspective is challenging due to the inherent complexity of individual types of events. In general, these events are usually a consequence of the intricate interplay between the local climate system, variability in large-scale circulation patterns, and even climate change. However, different sequences are driven by different physical processes and may exhibit contrasting responses to global warming. Specifically, D-to-W TCEs are usually associated with the disturbed energy budget and can be attributed to the impacts of global warming. As the climate continues to warm, increased evapotranspiration rates resulting from higher temperatures can lead to an elevated risk and frequency of drought conditions. Concurrently, the likelihood of localized heavy precipitation events leading to flooding is expected to rise in response to increased atmospheric instability and promote convective development due to increased evapotranspiration rates (Fowler et al. 2021; He and Sheffield 2020). Further abrupt transition from dry to wet extreme events may also be influenced by significant changes in large-scale thermodynamics, circulation shifts, and land-sea atmospheric feedbacks (Deng et al. 2020). In contrast, recurrent arrivals of tropical intraseasonal oscillations and meandering of subtropical jets may dynamically facilitate back-to-back occurrences of W-to-D TCEs and are common in coastal regions, including western Japan, northwest Australia, and southeast China (Chen et al. 2020; Liao et al. 2021; Wang et al. 2019). This is also evident from our study which shows non-significant probability of occurrence for W-to-D TCEs. Major tropical cyclones have the capability to cause destructive flooding and can result in prolonged periods of excessive heat that offset reduced ambient temperature, through the lagged (days to weeks) effects of tropical cyclones released diabatic heating on the strengthening of an upper-level anticyclone and stabilization of the atmospheric layer (Hart et al. 2007; McTaggart-Cowan et al. 2007; Parker et al. 2013). Increasingly uneven intraseasonal distribution of precipitation may also result in W-to-D TCEs via triggering a chain of process, i.e., a rapid swing from flash flood to drought first (Chen 2020; Pendergrass and Knutti 2018) and drought-fueled heatwaves afterward (Miralles et al. 2014). Further compelling scientific evidence of human interventions and land use changes such as increased human water consumption, urbanization, agricultural practices, and levee and dam construction could exacerbate the extreme drought and flood risk hazard (He et al. 2017; Munoz et al. 2018; Villarini and Strong 2014; Yang et al. 2013).

In the context of BC, none of the BC methods under both approaches retains the change signal of the raw counterparts for SPEI indices and TCEs except for CMIP6 ensemble where all BC methods show a slight preservation of raw climate change signals for the D-to-W TCEs in terms of spatial patterns. The probability and its statistical significance increased remarkably after all BC methods. Further, the BC methods under direct approach (i.e., D-EQM and D-QDM) modify to a larger extent the raw signals compared to MBCn whose signals are somewhat similar to those projected by BC methods under component-wise approach (i.e., CW-EQM and CW-QDM), especially for SPEI indices.

The comparable performance of the direct and component-wise approaches is evident in evaluation experiments with slightly better for direct approach (Ansari et al. 2023). However, remarkable differences in the climate change signals are found between both approaches with the direct correction introducing a greater modification of the original change signals especially for the SPEI indices, consistent with previous literature (Casanueva et al. 2018; Chen et al. 2021).

The similar climate change signals projected by MBCn and CW-QDM is primarily attributed by construction as MBCn uses QDM to adjust the marginal distributions of the individual variables and associated with the ability of univariate quantile mapping methods to implicitly adjust the joint probability distribution in a multivariate context (Casanueva et al. 2019). The small difference between the projected climate change signals by these two BC methods shows that the use of a multivariate BC method may not offer significant advantages over univariate BC methods. Ansari et al. (2023) also found little added value of multivariate BC methods during the evaluation step which may be due to the weak daily correlation between the considered variables (i.e., precipitation and temperature) in this region. Further, the present study found no remarkable difference between trend-preserving, i.e., QDM, and non-trend-preserving, i.e., EQM, under both approaches. Nevertheless, the absence of clear difference between these two BC methods in this study does not negate the potential benefits of trend-preserving BC over non-trend-preserving BC methods.

To summarize, it is anticipated that moderate to extreme wet and dry events will become more frequent and severe, with an increase in the frequency and severity up to eight events and 2.50 SPEI units relative to baseline period, respectively, by the end of the century. The duration of

extreme wet and dry events exhibits distinct change signals depending on the location. Further results indicate that the UJB is more prone to D-to-W TCEs than to W-to-D TCEs and identify the monsoon-dominated region located in the southwest of the basin as the hotspot for the D-to-W TCEs. Our results confirm the crucial importance of incorporating risk management strategies for potential TCEs into disaster risk reduction policies at the identified hotspots. The findings are of utmost relevance to a diverse group of decision-makers, including those responsible for managing dams and water resources. However, there remain several unanswered questions which need to be further explored. For instance, the characteristics of compound events such as severity, duration, spatial extent and seasonality and the possible physical mechanisms associated with them.

Supplementary information.

Supplementary Information The online version contains supplementary material available at https://doi.org/10.1007/s10113-025-02367-z.

Acknowledgements The authors acknowledge the World Climate Research Programme's Working Group on Regional Climate, and the Working Group on Coupled Modelling, former coordinating body of CORDEX and responsible panel for CMIP5. We also thank the climate modelling groups (listed in Tables 1 and 2 of Ansari et al. (2023)) for producing and making available their model output. We also acknowledge the Earth System Grid Federation infrastructure, an international effort led by the U.S. Department of Energy's Program for Climate Model Diagnosis and Intercomparison, the European Network for Earth System Modelling, and other partners in the Global Organisation for Earth System Science Portals (GO-ESSP). Data was accessed through the Santander Climate Data Service, which is maintained by the Santander Meteorology Group. The authors are also grateful to Ezequiel Cimadevilla (Santander Meteorology Group) for technical support and to George Zittis (Associate Editor) and the anonymous reviewer who helped to improve the original manuscript.

Author contribution R.A., A.C., and G.G. conceptualized the study. R.A. performed the formal analyses. A.C. gave support regarding the bias correction methods, model data, and compound events and M.U.L. provided ideas for new analyses and illustrations. G.G. and A.C. supervised the work. R.A. wrote the first draft of the paper, and all authors reviewed the text and contributed to the final version.

Funding Open Access funding provided thanks to the CRUE-CSIC agreement with Springer Nature. The first author as a PhD student received funding from the Cooperation Agreement PFK PhD program 2019–2022 "Partnership for Knowledge-Platform 2: Health and WASH (WAter Sanitation and good Hygiene)" of the AICS-Italian Agency for Development Cooperation to attend higher education programs in Italy in favor of non-Italian citizens. The first author also thanks the Erasmus Training ship Program which allowed a research stay of 3 months at the University of Cantabria, Spain. A.C. acknowledges support from Project COMPOUND (TED2021-131334A-I00) funded by MCIU/AEI/https://doi.org/10.13039/501100011033and by the European Union NextGenerationEU/PRTR.

Data availability The reference data (W5E5) are available for download at https://data.isimip.org/https://doi.org/10.5880/PIK.2019.023 and the climate model simulations from three initiatives (CORDEX, CORDEX-CORE, and CMIP6) used in this study are accessible via the Earth System Grid Federation (ESGF archive; https://esgf.llnl.gov).

Declarations

Competing interests The authors declare no competing interests.

References

Anderson W, Seager R, Baethgen W, Cane M, You L (2019) Synchronous crop failures and climate-forced production variability. Sci Adv 5:eaaw1976. https://doi.org/10.1126/sciadv.aaw1976

Ansari R, Grossi G (2022) Spatio-temporal evolution of wet–dry event features and their transition across the Upper Jhelum Basin (UJB) in South Asia. Nat Hazard 22:287–302. https://doi.org/10.5194/nhess-22-287-2022

Ansari R, Liaqat MU, Grossi G (2022) Evaluation of gridded datasets for terrestrial water budget assessment in the Upper Jhelum River Basin-South Asia. J Hydrol 613:128294. https://doi.org/10.1016/j.jhydrol.2022.128294

Ansari R, Casanueva A, Liaqat MU, Grossi G (2023) Evaluation of bias correction methods for a multivariate drought index: case study of the Upper Jhelum Basin. Geosci Model Dev 16:2055–2076. https://doi.org/10.5194/gmd-16-2055-2023

Ansari R, Liaqat MU, Grossi G (2024) Improving flood and drought management in transboundary Upper Jhelum Basin-South Asia. Sci Total Environ 945:174044. https://doi.org/10.1016/j.scitotenv.2024.174044

Archer DR, Fowler HJ (2008) Using meteorological data to forecast seasonal runoff on the River Jhelum, Pakistan. J Hydrol 361:10–23. https://doi.org/10.1016/j.jhydrol.2008.07.017

Azmat M (2015) Water resources availability and hydropower production under current and future climate scenarios: The case of Jhelum River Basin, Pakistan. Ph D thesis. https://doi.org/10.6092/polito/porto/2594956

Baldwin JW, Dessy JB, Vecchi GA, Oppenheimer M (2019) Temporally compound heat wave events and global warming: an emerging hazard. Earth's Future 7:411–427. https://doi.org/10.1029/2018EF000989

Bastos A, Orth R, Reichstein M, Ciais P, Viovy N, et al. (2021) Vulnerability of European ecosystems to two compound dry and hot summers in 2018 and 2019. Earth Syst Dy 12:1015–1035. https://doi.org/10.5194/esd-12-1015-2021

Beard G, Chandler E, Watkins A, Jones D (2011) How does the 2010–11 La Niña compare with past La Niña events. Bull Aust Meteorol Oceanogr Soc 24:17–20

Cannon AJ (2018) Multivariate quantile mapping bias correction: an N-dimensional probability density function transform for

climate model simulations of multiple variables. Clim Dyn 50:31–49. https://doi.org/10.1007/s00382-017-3580-6
Cannon AJ, Sobie SR, Murdock TQ (2015) Bias correction of GCM precipitation by quantile mapping: how well do methods preserve changes in quantiles and extremes? J Clim 28:6938–6959. https://doi.org/10.1175/JCLI-D-14-00754.1
Casanueva A, Bedia J, Herrera S, Fernández J, Gutiérrez JM (2018) Direct and component-wise bias correction of multi-variate climate indices: the percentile adjustment function diagnostic tool. Clim Change 147:411–425. https://doi.org/10.1007/s10584-018-2167-5
Casanueva A, Kotlarski S, Herrera S, Fischer AM, Kjellstrom T, et al. (2019) Climate projections of a multivariate heat stress index: the role of downscaling and bias correction. Geosci Model Dev 12:3419–3438. https://doi.org/10.5194/gmd-12-3419-2019
Chen Y (2020) Increasingly uneven intra-seasonal distribution of daily and hourly precipitation over Eastern China. Environ Res Lett 15:104068. https://doi.org/10.1088/1748-9326/abb1f1
Chen H, Wang S, Zhu J, Zhang B (2020) Projected changes in abrupt shifts between dry and wet extremes over China through an ensemble of regional climate model simulations. J Geophys Res Atmos 125:e2020JD033894. https://doi.org/10.1029/2020JD033894
Chen J, Arsenault R, Brissette FP, Zhang S (2021) Climate change impact studies: should we bias correct climate model outputs or post-process impact model outputs? Water Resour Res 57:e2020WR028638. https://doi.org/10.1029/2020WR028638
Consortium R, Inventory RG (2017) A dataset of global glacier outlines: version 6.0: Technical Report, Global Land Ice Measurements from Space, Colorado, USA. Digital Media 10. https://doi.org/10.7265/N5-RGI-60
Cowan T, Wheeler MC, de Burgh-Day C, Nguyen H, Cobon D (2022) Multi-week prediction of livestock chill conditions associated with the northwest Queensland floods of February 2019. Sci Rep 12:5907. https://doi.org/10.1038/s41598-022-09666-z
Cucchi M, Weedon GP, Amici A, Bellouin N, Lange S, et al. (2020) WFDE5: bias-adjusted ERA5 reanalysis data for impact studies. Earth Syst Sci Data 12:2097–2120. https://doi.org/10.5194/essd-12-2097-2020
Deng K, Jiang X, Hu C, Chen D (2020) More frequent summer heat waves in southwestern China linked to the recent declining of Arctic sea ice. Environ Res Lett 15:074011. https://doi.org/10.1088/1748-9326/ab8335
Déqué M (2007) Frequency of precipitation and temperature extremes over France in an anthropogenic scenario: model results and statistical correction according to observed values. Glob Planet Chang 57:16–26. https://doi.org/10.1016/j.gloplacha.2006.11.030
Donges JF, Schleussner C-F, Siegmund JF, Donner RV (2016) Event coincidence analysis for quantifying statistical interrelationships between event time series: on the role of flood events as triggers of epidemic outbreaks. Eur Phys J Spec Top 225:471–487. https://doi.org/10.1140/epjst/e2015-50233-y
Eyring V, Bony S, Meehl GA, Senior CA, Stevens B, Stouffer RJ, Taylor KE (2015) Overview of the Coupled Model Intercomparison Project Phase 6 (CMIP6) experimental design and organization. Geosci Model Dev Discuss 9(5):1937–1958. https://doi.org/10.5194/gmd-9-1937-2016
Fish MA, Done JM, Swain DL, Wilson AM, Michaelis AC, et al. (2022) Large-scale environments of successive atmospheric river events leading to compound precipitation extremes in California. J Clim 35:1515–1536. https://doi.org/10.1175/JCLI-D-21-0168.1
Fowler HJ, Lenderink G, Prein AF, Westra S, Allan RP, et al. (2021) Anthropogenic intensification of short-duration rainfall extremes. Nat Rev Earth Environ 2:107–122. https://doi.org/10.1038/s43017-020-00128-6
Gao Y, Hu T, Wang Q, Yuan H, Yang J (2019) Effect of drought–flood abrupt alternation on rice yield and yield components. Crop Sci 59:280–292. https://doi.org/10.2135/cropsci2018.05.0319
Gaupp F, Hall J, Hochrainer-Stigler S, Dadson S (2020) Changing risks of simultaneous global breadbasket failure. Nat Clim Chang 10:54–57. https://doi.org/10.1038/s41558-019-0600-z
Giorgi F, Jones C, Asrar GR (2009) Addressing climate information needs at the regional level: the CORDEX framework. World Meteorol Organ (WMO) Bull 58:175. https://cordex.org/wp-content/uploads/2012/11/cordex_giorgi_wmo-1.pdf
Gu L, Chen J, Yin J, Slater LJ, Wang HM, et al. (2022) Global increases in compound flood-hot extreme hazards under climate warming. Geophys Res Lett 49:e2022GL097726. https://doi.org/10.1029/2022GL097726
Gudmundsson L, Boulange J, Do HX, Gosling SN, Grillakis MG, et al. (2021) Globally observed trends in mean and extreme river flow attributed to climate change. Sci 371:1159–1162. https://doi.org/10.1126/science.aba3996
Hargreaves GH, Samani ZA (1985) Reference crop evapotranspiration from temperature. Appl Eng Agric 1:96–99. https://doi.org/10.13031/2013.26773
Hart RE, Maue RN, Watson MC (2007) Estimating local memory of tropical cyclones through MPI anomaly evolution. Mon Weather Rev 135:3990–4005. https://doi.org/10.1175/2007MWR2038.1
He X, Sheffield J (2020) Lagged compound occurrence of droughts and pluvials globally over the past seven decades. Geophys Res Lett 47:e2020GL087924. https://doi.org/10.1029/2020GL087924
He X, Wada Y, Wanders N, Sheffield J (2017) Intensification of hydrological drought in California by human water management. Geophys Res Lett 44:1777–1785. https://doi.org/10.1002/2016GL071665
Hersbach H, Bell B, Berrisford P, Hirahara S, Horányi A, et al. (2020) The ERA5 global reanalysis. Q Roy Meteorol Soc 146:1999–2049. https://doi.org/10.24381/cds.adbb2d47
Holgate C, Pepler A, Rudeva I, Abram N (2023) Anthropogenic warming reduces the likelihood of drought-breaking extreme rainfall events in southeast Australia. Weather Clim Extremes 42:100607. https://doi.org/10.1016/j.wace.2023.100607
Jones C (2010) CORDEX: a coordinated regional downscaling experiment. In AGU Fall Meeting Abstracts vol. 2010, pp A23F-01. Bibcode: 2010AGUFM.A23F..01J. https://ui.adsabs.harvard.edu/abs/2010AGUFM.A23F..01J/abstract
Kopp J, Rivoire P, Ali SM, Barton Y, Martius O (2021) A novel method to identify sub-seasonal clustering episodes of extreme precipitation events and their contributions to large accumulation periods. Hydrol Earth Syst Sci 25:5153–5174. https://doi.org/10.5194/hess-25-5153-2021
Kornhuber K, Coumou D, Vogel E, Lesk C, Donges JF, et al. (2020) Amplified Rossby waves enhance risk of concurrent heatwaves in major breadbasket regions. Nat Clim Chang 10:48–53. https://doi.org/10.1038/s41558-019-0637-z
Kreibich H, Van Loon AF, Schröter K, Ward PJ, Mazzoleni M, et al. (2022) The challenge of unprecedented floods and droughts in risk management. Nature 608:80–86. https://doi.org/10.1038/s41586-022-04917-5
Laudon H, Poléo AB, Vøllestad LA, Bishop K (2005) Survival of brown trout during spring flood in DOC-rich streams in northern Sweden: the effect of present acid deposition and modelled pre-industrial water quality. Environ Pollut 135:121–130. https://doi.org/10.1016/j.envpol.2004.09.023
Lewis SC, King AD, Perkins-Kirkpatrick SE (2017) Defining a new normal for extremes in a warming world. Bull Am Meteor Soc 98:1139–1151. https://doi.org/10.1175/BAMS-D-16-0183.1
Li D, Lettenmaier DP, Margulis SA, Andreadis K (2019) The role of rain-on-snow in flooding over the conterminous United States.

Water Resour Res 55:8492–8513. https://doi.org/10.1029/2019WR024950
Liao Z, Chen Y, Li W, Zhai P (2021) Growing threats from unprecedented sequential flood-hot extremes across China. Geophys Res Lett 48:e2021GL094505. https://doi.org/10.1029/2021GL094505
López-Moreno JI, Pomeroy J, Morán-Tejeda E, Revuelto J, Navarro-Serrano F, et al. (2021) Changes in the frequency of global high mountain rain-on-snow events due to climate warming. Environ Res Lett 16:094021. https://doi.org/10.1088/1748-9326/ac0dde
Mahmood R (2013) Assessment of climate change impact on water resources and hydropower in the Jhelum River Basin, Pakistan (Doctoral dissertation), Asian Institute of Technology, School of Engineering and Technology Thailand
McCarthy N, Kilic T, Brubaker J, Murray S, de la Fuente A (2021) Droughts and floods in Malawi: impacts on crop production and the performance of sustainable land management practices under weather extremes. Environ Dev Econ 26:432–449. https://doi.org/10.1017/S1355770X20000455
McTaggart-Cowan R, Bosart LF, Gyakum JR, Atallah EH (2007) Hurricane Katrina (2005). Part II: Evolution and hemispheric impacts of a diabatically generated warm pool. Mon Weather Rev 135:3927–3949. https://doi.org/10.1175/2007MWR2096.1
Messmer M, Simmonds I (2021) Global analysis of cyclone-induced compound precipitation and wind extreme events. Weather Clim Extremes 32:100324. https://doi.org/10.1016/j.wace.2021.100324
Miralles DG, Teuling AJ, Van Heerwaarden CC, Vilà-Guerau de Arellano J (2014) Mega-heatwave temperatures due to combined soil desiccation and atmospheric heat accumulation. Nat Geosci 7:345–349. https://doi.org/10.1038/ngeo2141
Mishra A, Alnahit A, Campbell B (2021) Impact of land uses, drought, flood, wildfire, and cascading events on water quality and microbial communities: a review and analysis. J Hydrol 596:125707. https://doi.org/10.1016/j.jhydrol.2020.125707
Mujumdar M, Bhaskar P, Ramarao M, Uppara U, Goswami M, Borgaonkar H, Chakraborty S, Ram S, Mishra V, Rajeevan M (2020) Droughts and floods. Assessment of climate change over the Indian region: a report of the Ministry of Earth Sciences (MoES), Government of India 117–141. https://doi.org/10.1007/978-981-15-4327-2_6
Munoz SE, Giosan L, Therrell MD, Remo JW, Shen Z, et al. (2018) Climatic control of Mississippi River flood hazard amplified by river engineering. Nat 556:95–98. https://doi.org/10.1038/nature26145
O'Neill BC, Kriegler E, Riahi K, Ebi KL, Hallegatte S, et al. (2014) A new scenario framework for climate change research: the concept of shared socioeconomic pathways. Clim Chang 122:387–400. https://doi.org/10.1007/s10584-013-0905-2
Owen LE, Catto JL, Stephenson DB, Dunstone NJ (2021) Compound precipitation and wind extremes over Europe and their relationship to extratropical cyclones. Weather Clim Extremes 33:100342. https://doi.org/10.1016/j.wace.2021.100342
Pachauri RK, Allen MR, Barros VR, Broome J, Cramer W, et al. (2014) Climate change 2014: synthesis report. Contribution of Working Groups I, II and III to the fifth assessment report of the Intergovernmental Panel on Climate Change. In: Pachauri R, Meyer L (eds). Geneva, Switzerland, IPCC, p 151
Panday PK, Thibeault J, Frey KE (2015) Changing temperature and precipitation extremes in the Hindu Kush-Himalayan region: an analysis of CMIP3 and CMIP5 simulations and projections. Int J Climatol 35:3058–3077. https://doi.org/10.1002/joc.4192
Parker TJ, Berry GJ, Reeder MJ (2013) The influence of tropical cyclones on heat waves in Southeastern Australia. Geophys Res Lett 40:6264–6270. https://doi.org/10.1002/2013GL058257
Parry S, Marsh T, Kendon M (2013) 2012: from drought to floods in England and Wales. Weather 68:268–274. https://doi.org/10.1002/wea.2152
Pendergrass AG, Knutti R (2018) The uneven nature of daily precipitation and its change. Geophysical Research Letters 45(11):980–911,988. https://doi.org/10.1029/2018GL080298
Qiao Y, Xu W, Wu D, Meng C, Qin L, et al. (2022) Changes in the spatiotemporal patterns of dry/wet abrupt alternation frequency, duration, and severity in Mainland China, 1980–2019. Sci Total Environ 838:156521. https://doi.org/10.1016/j.scitotenv.2022.156521
Raymond C, Horton RM, Zscheischler J, Martius O, AghaKouchak A, et al. (2020) Understanding and managing connected extreme events. Nat Clim Chang 10:611–621. https://doi.org/10.1038/s41558-020-0790-4
Ridder N, De Vries H, Drijfhout S (2018) The role of atmospheric rivers in compound events consisting of heavy precipitation and high storm surges along the Dutch coast. Nat Hazard 18:3311–3326. https://doi.org/10.5194/nhess-18-3311-2018
Rizzo ML, Székely GJ (2016) Energy distance. Wiley Interdiscip Rev: Comput Stat 8:27–38. https://doi.org/10.1002/wics.1375
Roxy MK, Ghosh S, Pathak A, Athulya R, Mujumdar M, et al. (2017) A threefold rise in widespread extreme rain events over central India. Nat Commun 8:1–11. https://doi.org/10.1038/s41467-017-00744-9
Sanjay J, Krishnan R, Shrestha AB, Rajbhandari R, Ren G-Y (2017) Downscaled climate change projections for the Hindu Kush Himalayan region using CORDEX South Asia regional climate models. Adv Clim Chang Res 8:185–198. https://doi.org/10.1016/j.accre.2017.08.003
Seneviratne SI, Zhang X, Adnan M, Badi W, Dereczynski C, et al. (2021) 11 Chapter 11: Weather and climate extreme events in a changing climate. https://doi.org/10.1017/9781009157896.013
Singh D, Seager R, Cook BI, Cane M, Ting M, et al. (2018) Climate and the global famine of 1876–78. J Clim 31:9445–9467. https://doi.org/10.1175/JCLI-D-18-0159.1
Singh J, Ashfaq M, Skinner CB, Anderson WB, Mishra V, et al. (2022) Enhanced risk of concurrent regional droughts with increased ENSO variability and warming. Nat Clim Chang 12:163–170. https://doi.org/10.1038/s41558-021-01276-3
Sutanto SJ, Vitolo C, Di Napoli C, D'Andrea M, Van Lanen HA (2020) Heatwaves, droughts, and fires: exploring compound and cascading dry hazards at the pan-European scale. Environ Int 134:105276. https://doi.org/10.1016/j.envint.2019.105276
Svoboda M, Hayes M, Wood D (2012) Standardized precipitation index: user guide. World Meteorological Organization, (WMO-No. 1090), Geneva. https://public.wmo.int/en/resources/library/standardized-precipitation-index-user-guide
Tebaldi C, Debeire K, Eyring V, Fischer E, Fyfe J, et al. (2021) Climate model projections from the scenario model intercomparison project (ScenarioMIP) of CMIP6. Earth Syst Dyn 12:253–293. https://doi.org/10.5194/esd-12-253-2021
Teichmann C, Jacob D, Remedio AR, Remke T, Buntemeyer L, et al. (2021) Assessing mean climate change signals in the global CORDEX-CORE ensemble. Clim Dyn 57:1269–1292. https://doi.org/10.5194/esd-12-253-2021
Themeßl MJ, Gobiet A, Heinrich G (2012) Empirical-statistical downscaling and error correction of regional climate models and its impact on the climate change signal. Clim Change 112:449–468. https://doi.org/10.1007/s10584-011-0224-4
Ul Hasson S, Pascale S, Lucarini V, Böhner J (2016) Seasonal cycle of precipitation over major river basins in South and Southeast Asia: a review of the CMIP5 climate models data for present climate and future climate projections. Atmos Res 180:42–63. https://doi.org/10.1016/j.atmosres.2016.05.008

van der Wiel K, Batelaan TJ, Wanders N (2023) Large increases of multi-year droughts in north-western Europe in a warmer climate. Clim Dyn 60:1781–1800. https://doi.org/10.1007/s00382-022-06373-3

Van Vuuren DP, Edmonds J, Kainuma M, Riahi K, Thomson A, et al. (2011) The representative concentration pathways: an overview. Clim Chang 109:5–31. https://doi.org/10.1007/s10584-011-0148-z

Vicente-Serrano SM, Beguería S, López-Moreno JI (2010) A multiscalar drought index sensitive to global warming: the standardized precipitation evapotranspiration index. J Clim 23:1696–1718. https://doi.org/10.1175/2009JCLI2909.1

Villarini G, Strong A (2014) Roles of climate and agricultural practices in discharge changes in an agricultural watershed in Iowa. Agr Ecosyst Environ 188:204–211. https://doi.org/10.1016/j.agee.2014.02.036

Visser-Quinn A, Beevers L, Collet L, Formetta G, Smith K, et al. (2019) Spatio-temporal analysis of compound hydro-hazard extremes across the UK. Adv Water Resour 130:77–90. https://doi.org/10.1016/j.advwatres.2019.05.019

Wang SSY, Kim H, Coumou D, Yoon JH, Zhao L, Gillies RR (2019) Consecutive extreme flooding and heat wave in Japan: Are they becoming a norm? Wiley Online Library, p e933. https://doi.org/10.1002/asl.933

Wang J, Li K, Hao L, Xu C, Liu J, et al. (2023) Disaster mapping and assessment of Pakistan's 2022 mega-flood based on multi-source data-driven approach. https://doi.org/10.1007/s11069-023-06337-8

Weedon GP, Balsamo G, Bellouin N, Gomes S, Best MJ, et al. (2014) The WFDEI meteorological forcing data set: WATCH Forcing Data methodology applied to ERA-Interim reanalysis data. Water Resour Res 50:7505–7514. https://doi.org/10.1002/2014WR015638

Wilcke RAI, Mendlik T, Gobiet A (2013) Multi-variable error correction of regional climate models. Clim Change 120:871–887. https://doi.org/10.1007/s10584-013-0845-x

Wurtsbaugh WA, Paerl HW, Dodds WK (2019) Nutrients, eutrophication and harmful algal blooms along the freshwater to marine continuum. Wiley Interdiscip Rev Water 6:e1373. https://doi.org/10.1002/wat2.1373

Yang L, Smith JA, Wright DB, Baeck ML, Villarini G, et al. (2013) Urbanization and climate change: an examination of nonstationarities in urban flooding. J Hydrometeorol 14:1791–1809. https://doi.org/10.1175/JHM-D-12-095.1

Zellou B, Rahali H (2019) Assessment of the joint impact of extreme rainfall and storm surge on the risk of flooding in a coastal area. J Hydrol 569:647–665. https://doi.org/10.1016/j.jhydrol.2018.12.028

Zhang B, Wang S, Zscheischler J (2021) Higher probability of abrupt shift from drought to heavy rainfall in a warmer world. https://doi.org/10.21203/rs.3.rs-940109/v1

Zhao Y, Weng Z, Chen H, Yang J (2020) Analysis of the evolution of drought, flood, and drought-flood abrupt alternation events under climate change using the daily SWAP index. Water 12:1969. https://doi.org/10.3390/w12071969

Zscheischler J, Fischer EM (2020) The record-breaking compound hot and dry 2018 growing season in Germany. Weather Clim Extremes 29:100270. https://doi.org/10.1016/j.wace.2020.100270

Zscheischler J, Martius O, Westra S, Bevacqua E, Raymond C, et al. (2020) A typology of compound weather and climate events. Nat Rev Earth Environ 1:333–347. https://doi.org/10.1038/s43017-020-0060-z